to appear in: Proceedings XI European Astronomy Meeting IAU,
Tenerife 3-8 July 1989, M. Vazquez Ed.

Chromospheric Phenomena in Late-Type Stars

P. ULMSCHNEIDER

Institut für Theoretische Astrophysik,
Universität Heidelberg,
Im Neuenheimer Feld 561
D–6900 Heidelberg, Federal Republic of Germany

Summary: Chromospheres and coronae are hot shell-like layers around stars which are characterized by strong H_α, Ca II, UV, IR and X-ray emission and by large spatial inhomogeneity. Chromospheres of late-type stars have a unique physics, where optically thick radiation fields with departures from thermodynamic equilibrium, strong magnetic fields, mechanical heating and mass flows dominate. In this short overview first the characteristic NLTE thermodynamics of chromospheres is discussed. Then the observational evidence for magnetic fields and their relation to the chromospheric emission activity of the sun and of stars (e.g. the magnetic field- radiative emission-, the rotation-activity-, the flux-flux- correlations, the two component theory, the upper and lower limits of chromospheric emission and the Wilson-Bappu effect) is summarized. A third unique feature of chromospheres and coronae is that they need persistent mechanical heating. Proposed heating mechanisms and in particular recent advances in acoustic heating are outlined. Finally the role of chromospheres and coronae in the generation of eruptive flows is discussed.

1. Introduction

Ground based and satellite observations have shown that probably all stars with the possible exception of A-stars have shells or regions in their outer atmosphere in which the temperature is much higher than the photospheric value. These chromospheric and coronal layers show a unique physics, distinctively different from the underlying photosphere and the overlying interstellar medium, which for late-type stars is characterized by four essential ingredients: 1. large departures from local thermodynamic equilibrium (NLTE) occur in the presence of optically deep radiation fields, 2. strong magnetic fields are present, 3. the energy balance is dominated by mechanical heating and 4. eruptive-type mass flows which can lead to stellar mass-loss are present. In the photosphere departures from LTE, magnetic fields (except in concentrated field areas like sunspots) and mechanical heating are not important, and one has only convective type flows. The interstellar medium has a NLTE thermodynamics with optically thin radiation fields, weak magnetic fields, no need of a persistent mechanical heating and exhibits different gas flows.

The physics of late-type chromospheres and coronae is also distinctively different from that of similar layers or regions in early-type stars which is dominated by intense radiation fields. The outer atmosphere of early-type stars is characterized by a NLTE thermodynamics, strong radiatively driven winds and by localized heating due to radiatively amplified acoustic shock waves. In Section 2 the NLTE thermodynamics of chromospheres and coronae is outlined, Section 3 deals with the solar and stellar magnetic fields and their relation with the chromospheric and coronal emission activity. Section 4 reviews the heating mechanisms and discusses why heating is necessary, while Section 5 describes mass flows generated in the chromospheres and coronae. The conclusions are presented in Section 6. Chromospheric phenomena have been reviewed recently by Linsky (1988), Hammer (1987) as well as Jordan and Linsky (1987), see also Linsky (1980) and Ulmschneider (1979).

2. Chromospheric NLTE thermodynamics

A characteristic property which is unique to chromospheres is encountered when one tries to construct empirical chromosphere models. Detailed models of the chromospheric temperature structure in the solar network and supergranulation cell interior are derived from UV continuum observations obtained from the Skylab space station (Vernazza et al. 1981). Assuming a run of temperature versus depth and enforcing hydrostatic equilibrium, an empirical model is constructed and the emergent intensity as function of wavelength is simulated. This run of temperature is subsequently varied such that the theoretical intensities optimally fit the observed intensities of the CI, SiI and HI continua. A characteristic property in this procedure is the strong departure from thermodynamic equilibrium (NLTE).

Assume two gas elements which have the same temperature: one deep in the photosphere and the other in the chromosphere (Fig. 1). Consider the energy levels and transition rates e.g. for the CI continuum. As for typical chromospheric temperatures the stimulated emission can be neglected for the UV continua, the radiative

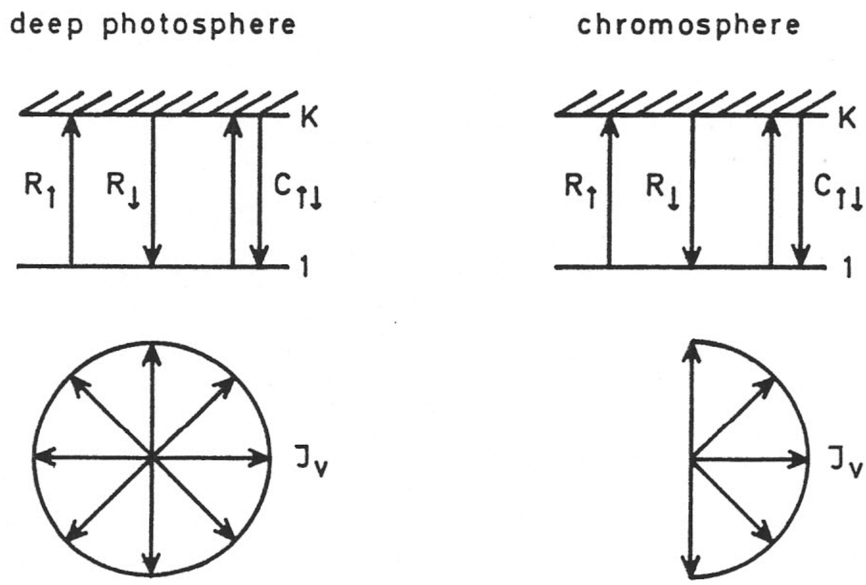

Fig. 1 Radiative and collisional transitions as well as the radiation field in chromospheric and deep photospheric gas elements.

recombination rate is given by $R_\downarrow = n_K(n_1^*/n_K^*)\int \alpha_1 \frac{4\pi}{h\nu}\frac{2h\nu^3}{c^2}\exp(-h\nu/kT)d\nu$ and the radiative absorption rate by $R_\uparrow = n_1 \int \alpha_1 \frac{4\pi}{h\nu} J_\nu d\nu$. Consider now the frequency integrals in $R_\downarrow$ and $R_\uparrow$. As we have the same temperature the frequency integrals for $R_\downarrow$ are the same, but for $R_\uparrow$ very different in the two gas elements. This is due to the fact that in the deep photosphere the mean intensity J_ν derives from an isotropic radiation field, while in the chromosphere only from the outwardly directed radiation field. With the collision rates $C_\uparrow = n_1 n_e \Omega_{1K}, C_\downarrow = n_K(n_1^*/n_K^*)n_e\Omega_{1K}$ one finds for the departure coefficient

$$b_1 = \frac{n_1}{n_1^*}\frac{n_K^*}{n_K} = \frac{\int \alpha_1 \frac{4\pi}{h\nu}\frac{2h\nu^3}{c^2} e^{-h\nu/kT} d\nu + n_e\Omega_{1K}}{\int \alpha_1 \frac{4\pi}{h\nu} J_\nu d\nu + n_e\Omega_{1K}} \quad , \tag{1}$$

where starred quantities are values in local thermal equilibrium (LTE). To enforce a balance between the radiative rates valid for statistical equilibrium, the rate $R_\uparrow$ must increase by overpopulating $n_1 = b_1 n_1^*(n_K/n_K^*)$ with $b_1 \approx 20$. An added difficulty is that J_ν is not a local function of height but must be computed solving the transfer equation using the NLTE source function S_ν:

$$J_\nu = \Lambda\{S_\nu\} \quad , \quad S_\nu = \frac{2h\nu^3}{c^2}\frac{1}{b_1 e^{h\nu/kT} - 1} \quad . \tag{2}$$

The *characteristic chromospheric difficulty* thus is a twofold one, that one needs to iterate between Eqs. (1) and (2) and that J_ν depends in a complicated way on the entire atmospheric structure. In the *transition layer and the corona* the thin plasma approximation applies, that is, radiative absorptions and return collisions can be neglected and Eq. (1) becomes a simple local function $b_1 = \int \alpha_1 \frac{4\pi}{h\nu}\frac{2h\nu^3}{c^2}\exp(-h\nu/kT)$ $d\nu/n_e\Omega_{1K}$ while in the *interstellar medium*, e.g. for planetary nebulae, the intensity in Eq. (1) is given by an optically thin value $J_\nu = WB_\nu$ where W is a dilution factor and $B_\nu(T_{eff})$ the Planck function of a very hot central star. Here with very low collision rates one then has $b_1 = \int \alpha_1 \frac{4\pi}{h\nu}\frac{2h\nu^3}{c^2}\exp(-h\nu/kT)d\nu / \int \alpha_1 \frac{4\pi}{h\nu} W B_\nu d\nu$, which again is a local function.

The described procedure was used to derive empirical chromosphere models for different solar surface regions from bright network elements to dark supergranulation cell interiors and plage areas (Vernazzza et al. 1981, Avrett 1985). In all models a rapid outward temperature increase was found with an almost discontinuous temperature rise in the transition region. Transition layer models have been constructed exploiting the thin plasma approximation discussed above and deriving emission measures from the transition layer line fluxes (Jordan and Brown 1981, Jordan et al. 1987). This way the chromospheric temperature structure can be followed to layers of increasing height in the lines L_α near 10^4 K, He II 304 Å near $2 \cdot 10^4$ K, C IV 1335 Å near 10^5 K to Mg X 625 Å near $2 \cdot 10^6$ K, the temperature maximum of the corona.

For stars other than the sun a large number of empirical chromosphere models have been constructed by reproducing the Ca II K and Mg II h+k line observations (see Linsky 1980), similarly as has been described above for the solar UV continuum observations. These models have the same characteristic difficulty with the NLTE thermodynamics as the continuum models, with the added problem that the line shape and the energy balance depend sensitively on the treatment of coherence in the line-wings (PRD). These problems are even more severe in time-dependent chromospheric wave calculations, for a review see Ulmschneider and Muchmore (1986). It should be pointed out that the above procedures to infer chromospheric temperatures depend on the assumption of a smoothly varying atmosphere and could be different if a very wavy atmosphere is assumed in which the emission occurs predominantly at the hottest parts of the wave (see Kalkofen et al. 1984).

The solar models of Vernazza et al. can be used to infer the chromospheric radiation losses which give a clue to the amount of mechanical heating necessary to support the chromosphere. As is shown in Section 4, persistent mechanical heating is absolutely essential to maintain both chromospheres and coronae. Vernazza et al. on basis of the empirical models identified the H^- continuum, and the Ca II, Mg II lines as the main chromospheric emitters. They also find, that the H_α losses are essentially balanced by radiative heating in the Balmer continuum. Recently Anderson and Athay (1989) have improved the computation of the net radiative cooling rate, Φ_R, by including FeII line losses. For the average chromosphere, Fig. 2, adopted from their work, shows Φ_R ($erg\ cm^{-3}\ s^{-1}$) as function of height together with the mechanical flux F_M which is obtained by integrating Φ_R over height. It is seen that a mechanical flux of about 10^7 $erg\ cm^{-2}\ s^{-1}$ at 400 km height is needed and that this flux at greater height decreases proportional to the gas pressure p, roughly like $F_M \approx 2.5 \cdot 10^9\ m \approx 9.2 \cdot 10^4\ p$, where m is the mass column density.

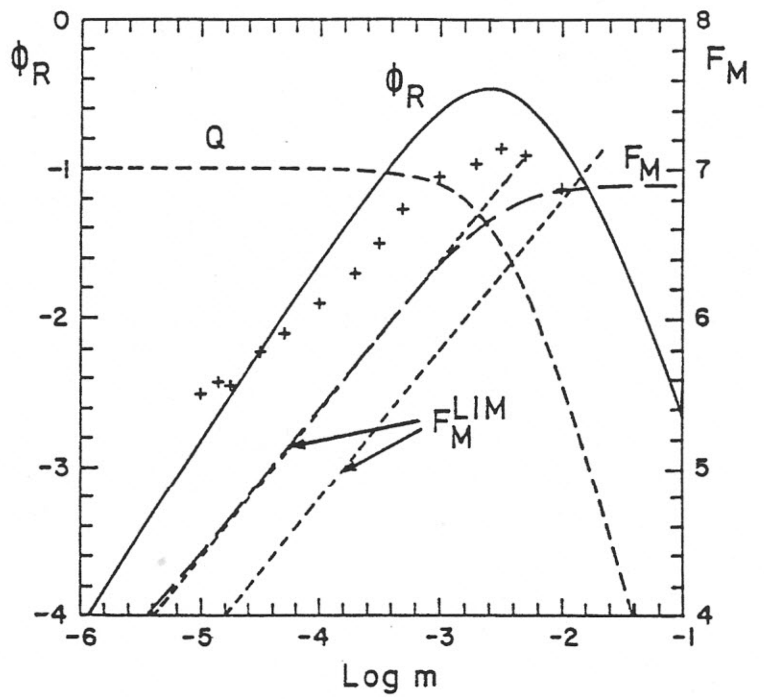

Fig. 2 Net radiative cooling rate Φ_R and mechanical Flux F_M after Anderson and Athay (1989), together with theoretical acoustic fluxes.

It is interesting that observations of short period (compared to the acoustic cut-off period P_A, see Eq. (7)) acoustic waves find energy fluxes of the same magnitude (Deubner et al. 1988) and that limiting strength acoustic shock waves have the same pressure dependence (see Section 4). Fig. 2 shows a comparison of the empirical F_M dependence with the theoretical limiting shock strength results of Eq. (8) for waves of period $P = 44,\ 22\ s$, where one has $F_M = 9.2 \cdot 10^4 p,\ 2.4 \cdot 10^4 p$, respectively.

3. Magnetic fields and chromospheric activity

Since about 10 years it is known that the solar surface is a two component medium with nonmagnetic areas where hot granulation cells come to the surface, and intense magnetic flux tubes concentrated in the intergranular lanes where the cool material flows back into the solar interior (Stenflo 1978, Zwaan 1978). The magnetic flux tubes are situated mainly on the boundaries of the supergranulation cells and in plage regions. Whether there are also flux tubes inside the supergranulation cell is presently controversial.

From observation one finds that the chromospheric emission e.g. in the Ca II H+K line cores is strongly concentrated in the magnetic areas above the supergranulation boundaries and plage regions. By detailed comparison of a Ca II K spectroheliogram and a magnetogram of an active region complex, Schrijver et al. (1989) have newly quantified the relation between the Ca II flux and the magnetic flux. They find

$$\Delta F_{CaII} = 0.6\ \log < fB > +4.8 \quad , \tag{3}$$

where f is the filling factor, B the magnetic field strength in G, and ΔF_{CaII} is the Ca II excess flux in $erg\ cm^{-2}\ s^{-1}$. Here $< fB >= \Phi/A$ where Φ is the measured average magnetic flux and A the area. The excess flux is computed by subtracting from the observed flux F_{CaII} the lower limit flux $F_{CaII\ LL}$ which consists of a non-magnetic photospheric radiative equilibrium contribution and a non-magnetic chromospheric basal flux contribution attributed to the heating by acoustic waves. For $F_{CaII\ LL}$ a stellar lower limit flux (see Fig. 3) was taken. This stellar lower limit is essentially identical to the flux $F_{CaII\ LL}$ observed from the supergranulation cell interior.

The X-ray and transition layer line emission, although more diffuse, also depends on the photospheric magnetic field. Similar as for the Ca II flux a correlation between the coronal X-ray emission flux and the magnetic flux has been inferred by Schrijver et al. (1985), Schrijver (1987a, 1989, Fig. 2) from a comparison of active regions of different size, quoted here after Vilhu (1987):

$$F_X = 4 \cdot 10^4 f\ B \quad . \tag{4}$$

Fig. 3 after Rutten (1987) shows the Ca II emission flux for dwarfs (dots) and giants (crosses) as function of colour. Note that all dwarfs of a given colour in a vertical slice in Fig. 3 are stars of the same kind, having the same effective temperature T_{eff} and gravity g. It is seen that these stars can have up to a factor of ten different Ca II emission fluxes which implies a corresponding difference in the magnetic flux coverage. Similar stars are thus shown to have a considerable *chromospheric emission variability.* Note, however, that towards small B-V this variability decreases markedly. Vaiana et al. (1981) show in their Fig. 5 a similar plot of X-ray emission flux versus spectral type for main sequence stars. Here the *X-ray emission variability* of three to four orders of magnitude for stars of the same T_{eff} and g is considerably larger.

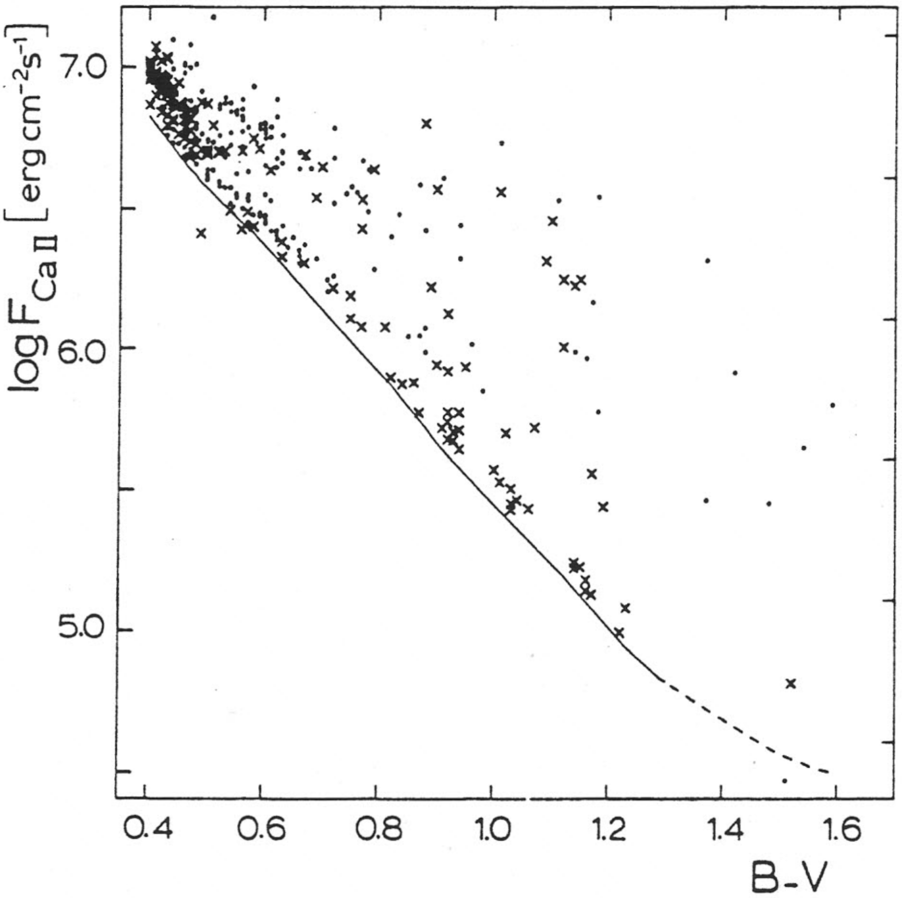

Fig. 3 Chromospheric emission fluxes F_{CaII} of stars versus colour after Rutten (1987). The drawn line is the lower limit flux $F_{CaII\ LL}$.

As shown in Fig. 4 after Rutten (1987) this chromospheric emission variability of late-type stars is due to the different rotation rates of similar kinds of stars. An X-ray flux-rotation relation of the same kind is shown in Fig. 5 of Pallavicini et al. (1981). These emission-rotation correlations are attributed to the dynamo mechanism. In the convection zones of late-type stars the dynamo mechanism leads to a greater magnetic flux generation the faster the stars rotate. In early- type stars there is no X-ray emission - rotation correlation but an X-ray emission - bolometric luminosity correlation as shown by Pallavicini et al. (1981, Figs. 2 and 3). Here the X-rays are generated in the hot regions behind strong acoustic shocks which have been amplified by the intense radiation field. For a recent review of the rotation-emission flux correlation and the evolution of rotation see Catalano (1989, this volume).

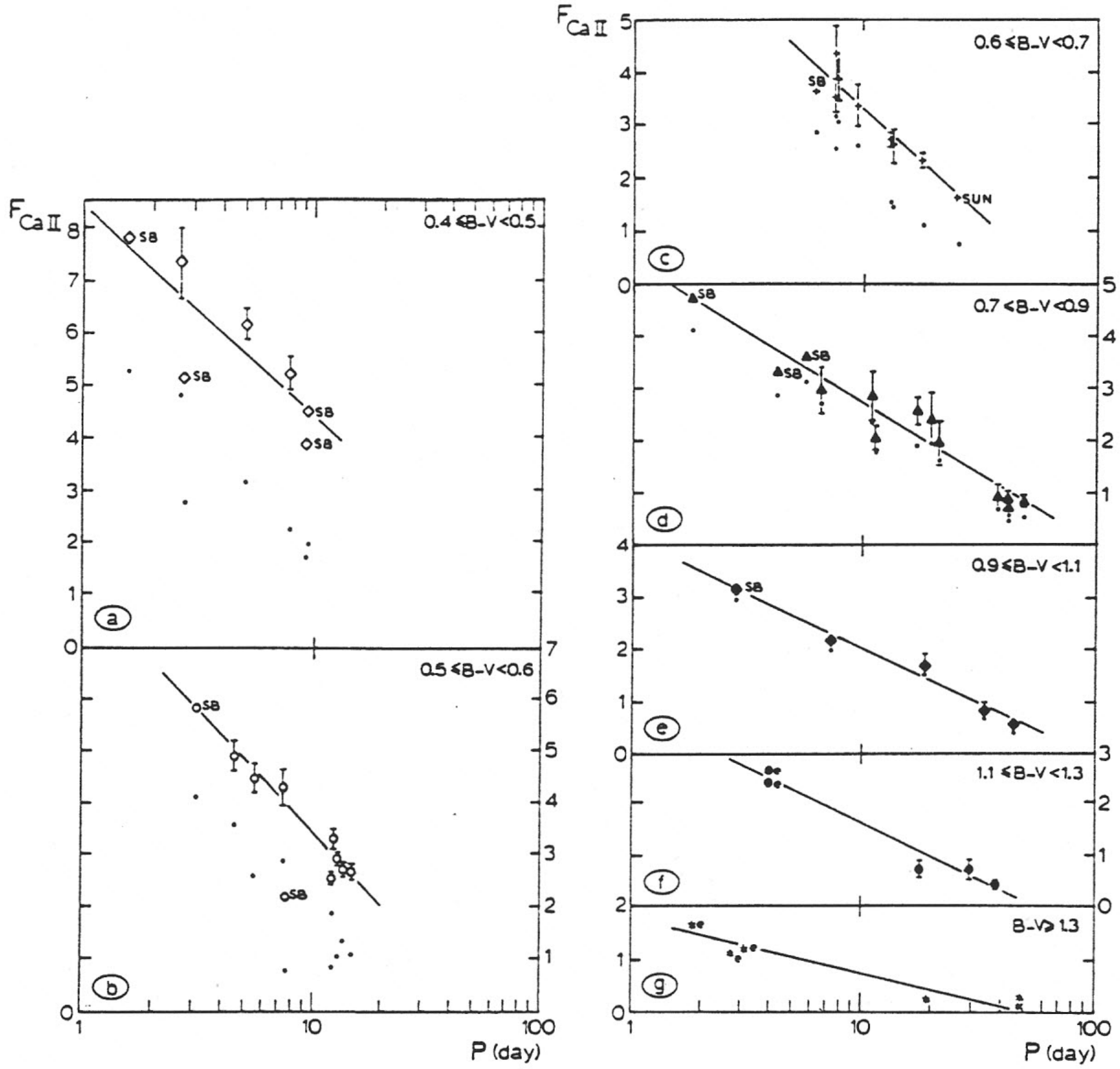

Fig. 4 Chromospheric emission fluxes F_{CaII} of stars versus rotation period for different colour intervals after Rutten (1986).

An interesting idea by Oranje and Zwaan (1985) and particularly by Schrijver (1987b) was to separate the chromospheric emission into two components: a *non-magnetic component* which is independent of rotation and only depends on T_{eff} and possibly slightly on g, and a *magnetic field related component* which depends on rotation. For late-type stars the heating by the nonmagnetic component leads to a *basal chromospheric emission flux* which is tentatively identified as due to the heating by acoustic shock waves. This basal flux constitutes a low background emission observable in stars of very low rotation rate but for faster rotating stars usually is greatly exceeded by the more energetic magnetic heating component.

The question is how to disentangle the nonmagnetic from the magnetic component, both for the sun and for stars? Stepien and Ulmschneider (1989) as well as Hammer and Ulmschneider (1989, see also Hammer 1989, this volume) show that pure acoustic wave heating either produces very weak coronae or no coronae at all. It thus appears that the coronal X-ray emission can only be produced by the magnetic field related heating component and should serve as an excellent indicator for the magnetic chromospheric emission component. It is thus not surprising that subtracting from the measured emission flux at a given colour the lowest observed emission flux from stars at this colour, Schrijver (1983) found that the correlation between the observed X-ray flux and e.g. the Ca II emission flux is considerably improved. The improvement of the magnetic field - Ca II flux correlation by subtracting a lower limit flux $F_{CaII\ LL}$ has already been discussed above.

The idea, that in the heating of chromospheres two components, a basal nonmagnetic, probably acoustic component and a magnetic, rotation dependent component are at work, can explain several other observations. We have already seen that for vanishing rotation only the nonmagnetic component survives which leads to the basal chromospheric emission. For Ca II after adding the unavoidable photospheric background line core and wing emission, one then finds the observed lower limit of the Ca II emission. For Mg II where the photospheric background is very weak the basal chromospheric emission is directly observed as lower limit flux. In the C IV and X-ray emission, arising in the transition layer and the corona, respectively, the observed lower limits are detection limits as shown by Schrijver (1987b).

Consider in Fig. 3 the low variability of the F-stars (see also Fig. 1 of Walter and Schrijver 1987). The theoretical acoustic energy generation computations of Bohn (1984) shown in Fig. 5 exhibit a strong increase towards higher T_{eff}. Although this calculation has been criticized, the general result, that earlier type stars as well as giants have more acoustic energy generation is not affected. This is a consequence of the fact that the acoustic energy generation depends on a high power of the convective velocity u. In fairly efficient convection zones one has $\sigma T_{eff}^4 \approx \rho u^3$, that is, the total stellar flux is carried mainly by the convective flux. As the convective velocity of stars is greatest near the surface where the densities are lowest, the acoustic energy generation is large only in the surface layers. Consequently acoustic energy generation does not depend on the depth of the stellar convection zone. Despite the fact that F-stars have shallow convection zones, the fact that in these stars T_{eff} is largest, before the convection zones disappear towards earlier spectral type, ensures that F-stars have the largest amount of acoustic energy production. Going towards earlier type stars, one thus adds an increasingly stronger acoustic heating component to a given variable magnetic heating component, which results in a reduced variability of the total emission.

By the same token as seen in Fig. 5, the acoustic energy generation increases when going from dwarfs to giants, because the density in the atmospheres of giant stars is much smaller than in dwarfs, and thus requires larger convective velocities to transport the same total flux σT_{eff}^4. From this one would expect a higher basal flux limit for giants than for dwarfs. Actually observations show the opposite, that the dwarfs appear to have a slightly higher basal flux limit than the giants (Schrijver

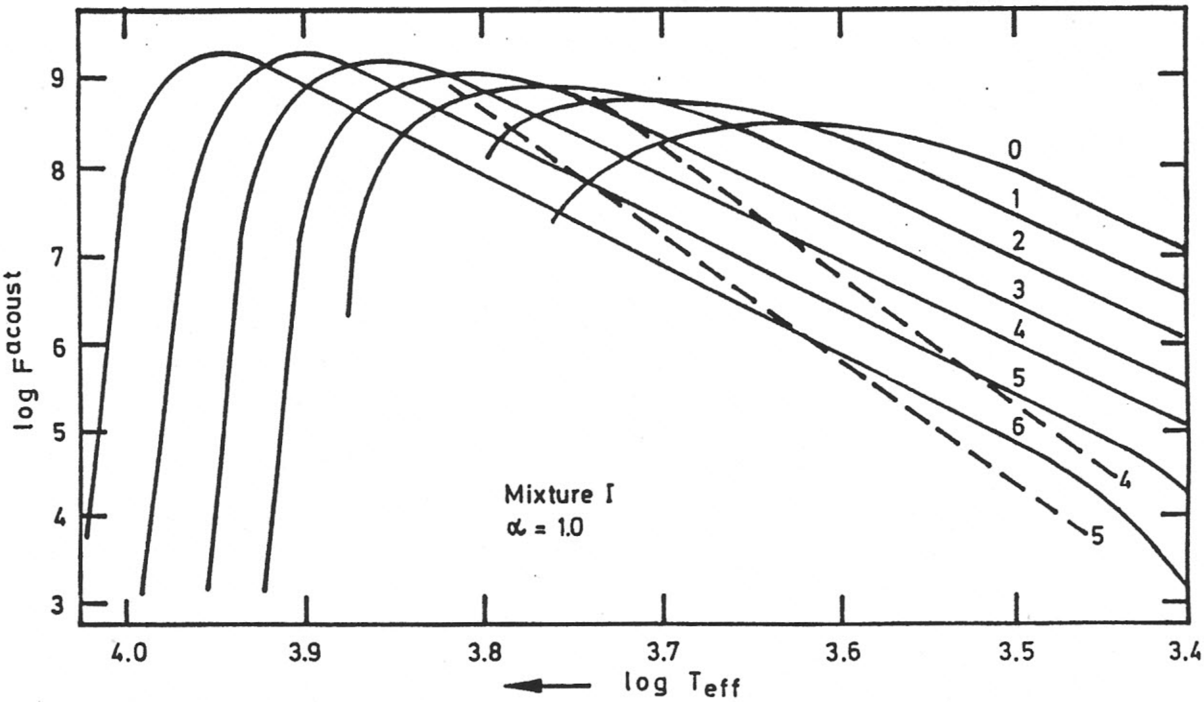

Fig. 5 Theoretical acoustic energy fluxes generated in stellar surface convection zones versus $\log T_{eff}$ *with* $\log\ g$ *as parameter after Bohn (1984).*

et al. 1989). Ulmschneider (1988, 1989) has shown that this can be explained by greater radiation damping of the acoustic waves in the giants and by the limiting shock strength behaviour of the acoustic waves, which leads to a lower limiting acoustic flux due to the lower gas pressure in giant star atmospheres.

Red giant stars, due to their low rotation rate resulting from angular momentum conservation during the large evolutionary increase in radius and from angular momentum loss by massive stellar winds, are another class of stars, where the two component chromospheric heating theory can be tested. Middelkoop (1982, Fig. 4a-c) showed that the chromospheric emission variability decreases very much toward late spectral type and there becomes a low basal emission. The same was found by Judge (1989) who studied late-type giants with peculiar chemical abundances. These are highly evolved stars in their red giant and AGB evolutionary state. Judge finds that these late M- and C-stars (the latter after correction for the Mg II circumstellar shell absorption) all fall on the same emission versus T_{eff} relation and do not show a chromospheric emission variability, consistent with the fact that in these stars only the nonmagnetic acoustic heating component seems to be present.

If one now considers the other extreme, the very quickly rotating stars, it is found that these stars approach an *upper limit of the chromospheric emission.* In Fig. 6 after Vilhu (1987) it is seen that this limit (dashed) is populated by different types

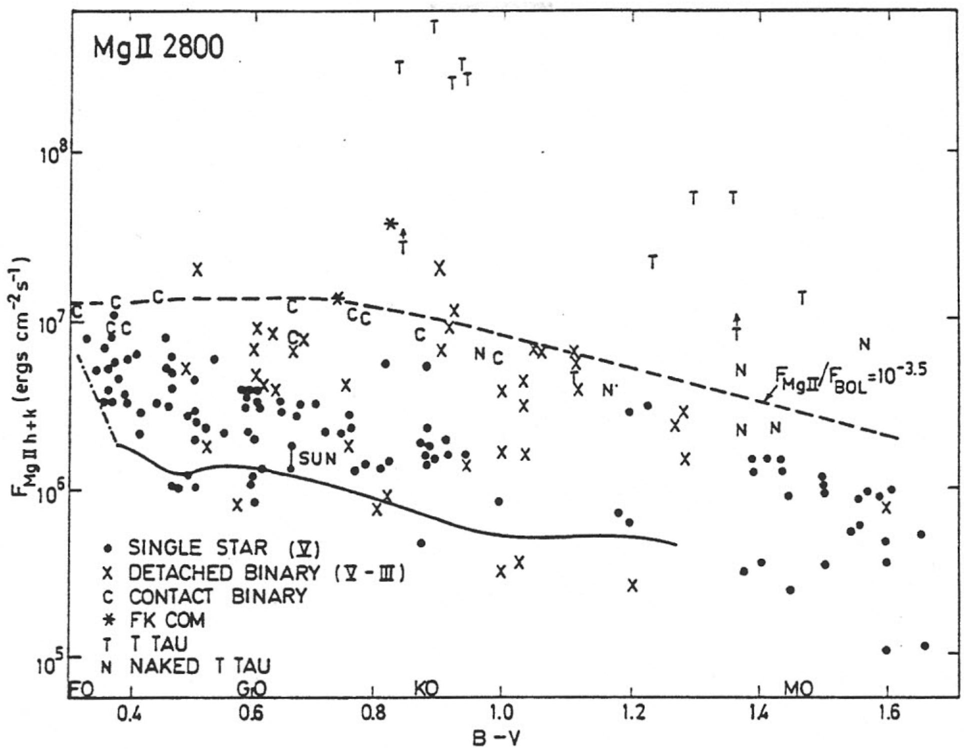

Fig. 6 Upper limit of the chromospheric emission flux F_{MgII} versus colour after Vilhu (1987).

of binaries where, the fast stellar rotation is apparently produced by tidal interaction between the binary stars. From the chromospheric emission - magnetic flux correlation it is clear that there must be a saturation, where the surface of the star is nearly completely filled by magnetic fields, that is, where the filling factor of the magnetic field is nearly one. This is supported by X-ray observation which also show a distinctive upper limit for rapidly rotating stars. Vilhu (1987, Fig. 5) showed that this X-ray flux agrees well with the solar relation found by Schrijver given above (Eq. 4) for a filling factor $f = 1$ and a field strength $B = 2000$ G.

It is interesting that Fig. 6 shows stars with Mg II emission larger than the upper limit. These stars are T-Tau stars where the emission comes from the innermost part of an accretion disk around these young stars. Here the energy which balances the chromospheric radiation losses is derived from mass accretion and not from the stellar convection zone inside the star. Note that the naked T-Tau stars, which apparently have lost their accretion disk, fall again on the upper limit for rapidly rotating stars.

Another interesting chromospheric effect is the well known Wilson-Bappu effect. Wilson and Bappu (1957) discovered that there is a tight correlation between the width of the Ca II K line emission core and the absolute visual magnitude of the stars which extends over roughly 15 magnitudes and is nearly independent of the emission strength of the line. A similar Wilson-Bappu relation has been found for the MgII k line (Elgarøy 1988). Hammer (1987) has recently reviewed the discussion on the origin of the Wilson-Bappu effect and concludes that several processes could produce this effect and that therefore the effect appears unpredictive as far as the heating mechanisms are concerned.

4. Mechanical heating

Stellar chromospheres and coronae are layers with persistent mechanical heating. Let us first discuss why chromospheres and coronae constantly require mechanical heating. Consider a chromospheric gas element. Due to the solar wind this element will slowly move and also exchange energy with its surroundings. A powerful book-keeping quantity for monitoring energy exchange is the entropy S $[erg\ g^{-1}\ K^{-1}]$, which in chromospheres changes mainly due to mechanical heating and radiation. In transition layers and coronae, thermal conduction, viscous- and Joule heating as well as other mechanisms described below are at work. From the second law of thermodynamics the energy equation describing the heat addition to a chromospheric gas element can be written

$$\rho T \left(\frac{\partial S}{\partial t} + \mathbf{v} \cdot \nabla S \right) = \Phi_M - \Phi_R \quad , \tag{5}$$

where ρ is the density, T the temperature, $\mathbf{v}$ the flow speed, $\Phi_M [erg\ cm^{-3}\ s^{-1}]$ the mechanical heating rate and Φ_R the radiative cooling rate. For illustration let us assume grey radiation, then we have $\Phi_R = 4\pi\kappa(B - J)$, where κ is the absorption coefficient, B the frequency integrated Planck function and J the mean intensity. Other expressions for Φ_R are given by Ulmschneider and Muchmore (1986).

Since the chromosphere has not changed much over millions of years we can consider it as a steady state phenomenon and have $\partial S/\partial t = 0$. The entropy gradient can be approximated by $dS/dx = g/T$, valid for an isothermal atmosphere. For the heating due to the potential energy flux one then gets $\rho T \mathbf{v} \cdot \nabla S = \rho v g \approx 8 \cdot 10^{-7}\ erg\ cm^{-3}\ s^{-1}$. Here $\rho \approx 4 \cdot 10^{-11}\ g/cm^3$ and $v \approx 0.75\ cm/s$, were used for the middle chromosphere. Compared with the value $\Phi_R \approx 0.3$ found by Anderson and Athay (1989) (see Fig. 2), the left hand side of Eq. (5) can thus be safely neglected and there remains a balance between mechanical heating and radiative cooling.

Let us suppose for a moment that there is no mechanical heating. Then radiative equilibrium prevails, and one has in the grey case $B = J$. With $B = \sigma T^4/\pi$ and $J = \frac{1}{2}\sigma T_{eff}^4/\pi$, where the factor 1/2 takes into account that there is only outgoing radiation, one finds $T^4 \approx \frac{1}{2}T_{eff}^4$ or $T \approx 0.8 T_{eff}$. This is the well known result that grey radiative equilibrium atmospheres have a boundary temperature with $T < T_{eff}$. From the empirical chromospheric and coronal temperature distributions of Section 1 with $T >> T_{eff}$ it is thus clear that *mechanical heating is absolutely essential* and that in Eq. (5) one can neglect the radiative heating term $4\pi\kappa J$, and has a balance of mechanical heating and radiative cooling, $\Phi_M = 4\pi\kappa B$. The heating moreover must be *constantly* applied, because if it were switched off, then the chromosphere would rapidly cool down to the boundary temperature at a time scale of the radiative damping time $t_{rad} = \rho c_v/(16\kappa\sigma T^3) \approx 200\ s$. Here c_v is the specific heat at constant volume. For the corona one finds $t_{rad} = \rho c_v T/(7 \cdot 10^{-17} T^{-1} n^2) \approx 4.3 \cdot 10^3\ s \approx 1\ h$ for the radiative damping alone, while thermal conduction decreases this time further. Here we have assumed the thin plasma approximation with $T \approx 2.5 \cdot 10^6\ K$ and $n \approx 2 \cdot 10^9\ cm^{-3}$.

The mechanisms which have been proposed to heat the chromosphere and corona have recently been summarized by Narain and Ulmschneider (1989). Tab. 1 gives a list of these mechanisms.

mechanism	**dissipation**
acoustic waves	shock dissipation
slow-mode mhd waves	shock dissipation
fast-mode mhd waves	Landau damping
Alfvén waves	mode-coupling
	resonant heating
	turbulent heating
	Landau damping
	phase mixing*
	resonant absorption*
current heating	Joule heating
	reconnection
	turbulent heating

*Table 1 Chromospheric and coronal heating mechanisms and their mode of dissipation. Dissipation modes labeled * depend on transverse Alfvén speed variations.*

We first discuss the acoustic heating mechanism. Here acoustic waves generated in the stellar surface convection zone run down the steep density gradient of the outer stellar atmosphere and, due to energy conservation, grow to large amplitude and form shocks. Acoustic wave heating is due to shock dissipation, while direct viscous and thermal conductive heating is unimportant. There are two effects which severely influence the behaviour of acoustic waves. First, the acoustic wave energy flux is strongly affected by *radiation damping*, when the wave propagates through the radiation damping zone, which in the sun extends to heights of about 200 km, but for other stars can be much more extended (Ulmschneider 1988). Second, it is a persistent result of time-dependent acoustic wave calculations that acoustic shock waves, once formed, tend to quickly reach *limiting shock strength.*

This behaviour, where the wave amplitude becomes essentially constant with height, and independent from the initial amplitude, results from the balance of shock dissipation which decreases the wave amplitude and amplitude growth which is caused by the steep density gradient (Ulmschneider 1970, Cuntz and Ulmschneider 1988, Ulmschneider 1989). In an isothermal atmosphere the limiting shock strength is given by (Ulmschneider 1970)

$$M_S^{Lim} = 1 + \frac{\gamma g}{4 c_S} P \quad , \tag{6}$$

where $\gamma = 5/3$ is the ratio of specific heats, $c_S(T_{eff})$ the sound speed and P the wave period. After the calculations of Bohn (1984) the acoustic wave spectrum generated by the turbulent motions in the stellar convection zone extends from the acoustic cut-off period P_A roughly 1.5 decades to shorter wave periods with a maximum near $P_A/10$. This maximum shifts towards $P_A/5$ and longerwards for late type dwarf stars. Thus acoustic waves typically have wave periods of

$$P = \frac{1}{10} P_A = \frac{1}{10} \frac{4\pi c_S}{\gamma g} \quad . \tag{7}$$

From Eqs. (6) and (7) one has $M_S^{Lim} = 1.3, 1.6$ for $P = P_A/10, P_A/5$, respectively. Note that this result is roughly valid for all late-type stars, independent of gravity and T_{eff}. Consequently the velocity-, temperature- and pressure amplitudes of limiting acoustic shock waves are also roughly the same for all late-type stars. With $v \approx 2c_S(M_S^{Lim} - 1)/(\gamma + 1) \approx 0.23 c_S$ one finds

$$F_M^{Lim} = \frac{1}{3}\rho v^2 c_S \approx 2.4 \cdot 10^4 \ p \quad , \tag{8}$$

for $P = P_A/10$, or $F_M^{Lim} \approx 9.2 \cdot 10^4 \ p$ for $P = P_A/5$. These limiting acoustic wave fluxes, which are roughly valid for all late-type stars, have been plotted in Fig. 2.

Slow-mode mhd waves in homogeneous fields and longitudinal mhd tube waves in magnetic flux tubes, in situations where the Alfvén speed, $v_A > c_S$, are essentially acoustic waves propagating along the magnetic field (Herbold et al. 1985). They very likely are an important heating mechanism for the lower and middle chromosphere (see Ulmschneider 1986). In addition to the direct generation of these waves in the convection zone they are also generated in the chromosphere and corona from transverse or torsional Alfvén waves by mode-coupling. Like acoustic waves, they heat by shock dissipation. From the acoustic nature of these waves it is clear that they suffer radiation damping and show the limiting shock strength behaviour (Herbold et al. 1985), when they travel along magnetic flux tubes with slowly varying cross- section (e.g. tubes where the field has fully spread over the available space).

Fast-mode mhd waves due to the strongly increasing Alfvén speed in the upper chromosphere are thought to be strongly refracted away from the high chromosphere and thus do not form shocks. However, the generation by mode-coupling of these waves in the corona, their property to refract away from regions of high Alfvén speed and to dissipate by Landau damping could be important for the explanation of coronal loops with cool cores (Habbal et al. 1979).

Transverse and torsional Alfvén waves are pure shear waves and to first order do not show temperature or density fluctuations. Consequently they do not suffer from radiation damping. They are also not easily dissipated in the chromosphere by simple Joule heating, viscous- or ion-neutral collisional heating. As they are thought to be efficiently generated in the convection zone (Ulmschneider 1986), these waves should carry a considerable energy into the upper chromosphere, corona and the solar wind (Withbroe 1988). A surprising number of more complex, nonlinear processes, some of which derived from heating experiments in plasma fusion, have been proposed to dissipate Alfvén waves (Tab. 1). Yet most of these very promising dissipation mechanisms have presently not been investigated enough to give detailed predictions in specific chromospheric or coronal loop situations. Only order of magnitude estimates are presently available for most mechanisms showing their viability (see Narain and Ulmschneider 1989).

Mode-coupling is an efficient and very general method by which mhd waves in the complex coronal magnetic field geometry generate other types of mhd waves. Fig. 7 from Ulmschneider et al. (1989, see also Zähringer and Ulmschneider 1987) is an illustrative example. Here a thin, vertically directed solar magnetic flux tube has been excited at the bottom by purely transverse shaking. The restoring forces are due to the tension of the magnetic field and are directed towards the center of curvature of the magnetic field distorted by the wave (c.f. Fig. 7). The curvature forces can be divided into vertical and horizontal components of which the horizontal components drive the pure transverse Alfvén wave and the vertical components lead to compression and expansion of the gas in the flux tube, that is, generate a longitudinal tube wave. It is easy to visualize related situations where mode-coupling should occur: bent magnetic loops (Wentzel 1974) or magnetic loops meeting adjacent magnetic fields must lead to deformations of the gas columns or sheets and thus give rise to acoustic-type waves which subsequently are easily dissipated by shocks.

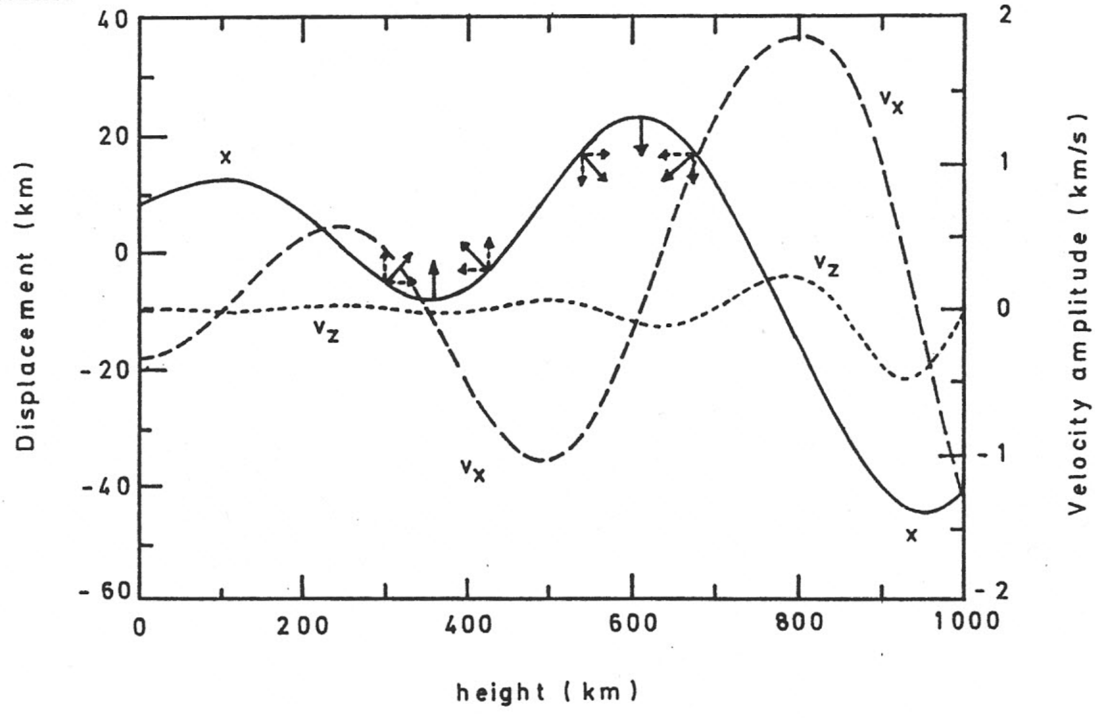

Fig. 7 Longitudinal-transverse mhd tube wave initiated by purely transverse shaking at the bottom. The components of the curvature force vector are shown. x is the horizontal displacement, v_x and v_z are the horizontal and vertical velocity components.

Resonant heating lives from the reflection of Alfvén waves at the foot points of a coronal loop which is very analogous to the situation in an electric resonant circuit (Ionson 1984). From a wide spectrum of Alfvén waves generated in the convection zone, similarly to an electric circuit, only those waves which are in a narrow band around the resonant frequency get absorbed.

Turbulent heating possibly is a very promising method for the dissipation of Alfvén wave energy but also for the magnetic energy stored at much slower time scales (see current heating below). Here the magnetic field perturbations in the closed or open coronal flux tubes are supposed to be dissipated by turbulence developing perpendicular to the tube axis. Dahlburg et al. (1988) have recently performed three-dimensional time- dependent numerical simulations in a vertical coronal gas column, which show this effect and the ensuing formation of current sheets where reconnection takes place and vortex structures where viscous dissipation occurs.

Phase-mixing and resonant absorption are processes which live from a transverse Alfvén speed gradient of the coronal flux tube. After coherent transverse shaking at the foot point of the tube, the transverse Alfvén speed variation leads to a variation of the phase speed (phase-mixing) in adjacent field lines resulting in the build-up of transverse magnetic field gradients which results in current sheets and reconnective heating (Heyvaerts and Priest 1983). Resonant absorption occurs, when at a certain magnetic field line the Alfvén speed matches the phase speed of the Alfvénic surface wave which travels in the loop boundary region where there is a transverse Alfvén speed variation. In a narrow layer around the resonant field line considerable energy dissipation occurs (Ionson 1978). Resonant absorption should not be confused with resonant heating discussed above, which is due the constructive interference from waves reflected at the photospheric foot points of a coronal loop. While resonant heating occurs only in loops, resonant absorption also occurs in open structures. In realistic situations loop resonances and resonant absorption occur simultaneously as has been shown by Grossmann and Smith (1988), who studied the resonant absorption of a photospheric spectrum of Alfvén waves in coronal loops.

Slow photospheric footpoint motions with timescales much longer than the loop transit timescales can store large amounts of magnetic energy in coronal loops which is thought to be dissipated by currents flowing along the magnetic field. In addition these motions lead to interweaving and winding magnetic field filaments (Van Ballegooijen 1986). In both cases the currents are unsteady and associated with reconnection and turbulent heating as discussed above. It is widely assumed that the current heating processes correspond to micro- and nanoflare events (see Section 5).

5. Mass flows

The fourth essential characteristic of chromospheres and coronae is that they are layers where mass flows and mass loss originate. A well known mass flow phenomenon on the sun are the *spicules* (Beckers 1972). Observed mainly on the solar limb, spicules are jets of cool plasma with temperatures of $T_{sp} \approx 1.5 \cdot 10^4\ K$ protruding into the hot corona, which rise with velocities of $v_{sp} \approx 20\ km/s$. The lifetime of spicules is about 1/2 hr. Athay and Holtzer (1982) estimated that with a density of $n_{sp} \approx 6 \cdot 10^{10}\ cm^{-3}$ and an area filling factor of $A_{sp} \approx 0.01$ a particle flux density of $F_{sp} = n_{sp}v_{sp}A_{sp} \approx 1.2 \cdot 10^{15}\ cm^{-2}\ s^{-1}$ of cool spicular material enters the corona. This is about a factor 100 more than the particle flux density of the solar wind of $F_{wind} = 1.4 \cdot 10^{13}\ cm^{-2}\ s^{-1}$, which shows that most of the spicular mass must return to the sun. The question is how. As there is little doubt that the spicular flow is along magnetic loops, the question is whether the spicular flow goes up one leg of the loop and comes down the other leg, as is proposed by the so called siphon flow models, or whether it comes down the same leg as is supposed by the eruptive flow models. In any case the spicular material is rapidly heated and comes down as gas of transition layer temperature.

Systematic *downflows* with velocities of $v \approx 4 - 17\ km/s$ have been observed in UV lines by Doschek et al. (1976), Brueckner (1981), Gebbie et al. (1981) and Feldman et al. (1982) particularly in the transition layer line C IV at temperatures of $T \approx 10^5\ K$. Athay and Holtzer (1982) assuming a downflow velocity of $v_{df} \approx 4\ km/s$, a particle density $n_{df} \approx 6 \cdot 10^9\ cm^{-3}$ and an area filling factor of $A_{df} \approx 0.45$, find a particle flux density of $F_{df} = n_{df}v_{df}A_{df} \approx 1.1 \cdot 10^{15}\ cm^{-2}\ s^{-1}$ in the downflows which agrees well with the spicular mass flow. The observation of double neutral lines in C IV dopplergrams moreover shows that the eruption model appears to be the correct picture with siphon flows occurring only occasionally (Athay et al. 1983, Athay 1987).

Mass flows do not depend on collimating magnetic fields, but as a result of a stochastic production of acoustic energy, can also occur in nonmagnetic situations over certain areas of the stellar surface. Cuntz (1987) describes episodic mass loss events in late-type giant stars which are caused by the nonlinear interaction of a stochastic field of acoustic shock waves. Fig. 8 shows how a slightly faster shock of small amplitude from a spectrum of acoustic shock waves catches up with the shock propagating in front and thereby strengthens to a larger shock. The now even more quickly moving shock eats up more shocks in front and eventually by cannibalizing a large number of shocks grows to large amplitude which leads to episodic mass loss.

Two different types of flows called *turbulent events* and *high velocity jets* have been observed by Brueckner and Bartoe (1983) in the corona above the quiet sun. Turbulent events are confined to small areas ($< 1500\ km$) and have average lifetimes of 40 s. The average energy of a turbulent event is $7 \cdot 10^{23}\ erg$. With 753 events per sec one has a heating flux of $9 \cdot 10^3\ erg\ cm^{-2}\ s^{-1}$ for the whole sun in turbulent events. High-velocity jets have moving material with velocities ($\approx 400\ km/s$) exceeding the sound speed ($\approx 120\ km/s$) and are confined to areas $< 3000\ km$. A single jet with an energy of $3 \cdot 10^{26}\ erg$ carries a mass of $3 \cdot 10^{11}\ g$ to an altitude of $4000 - 16000\ km$ and has a maximum lifetime of 80 s. With 24 jets per second one finds a heating flux of $1 \cdot 10^5\ erg\ cm^{-2}\ s^{-1}$ over the whole sun.

Parker (1983, 1986, 1988) suggests that the turbulent events and high velocity jets are only the tip of the iceberg of a large number of events which are associated with the heating of the corona by reconnective dissipation at many small current sheets

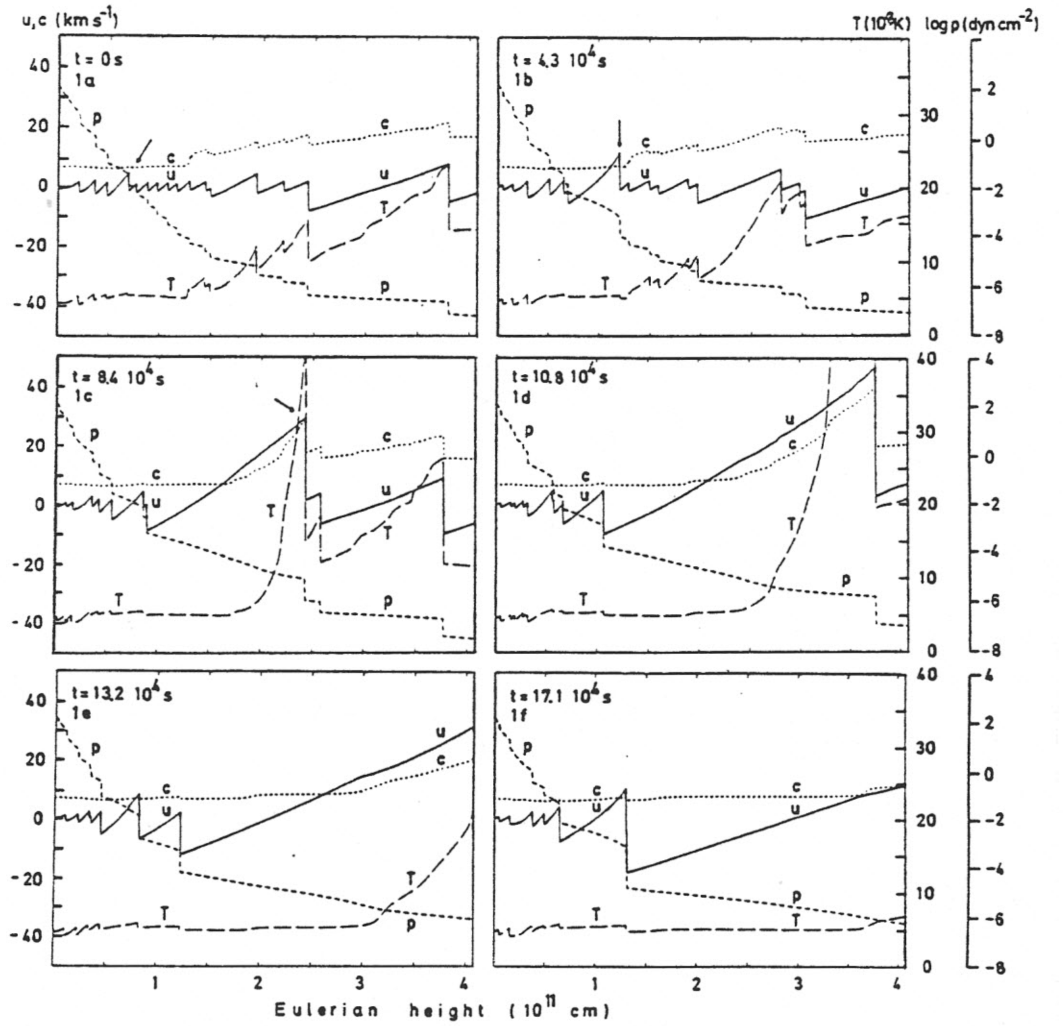

Fig. 8 Shock overtaking for a spectrum of acoustic shock waves in late-type giant star atmospheres after Cuntz (1987).

which are formed all the time as tangential discontinuities between interweaving and winding magnetic filaments. The individual reconnection events are called *nanoflares.* From Si IV and O IV emission line fluctuations and using an estimate of the heating flux of $1 \cdot 10^7$ $erg\ cm^{-2}\ s^{-1}$ for active regions by Withbroe and Noyes (1977), Parker estimates that there are about $8 \cdot 10^6$ nanoflares per sec over the whole sun with powers of 10^{23} erg/s each and a lifetime of 20 s. The largest nanoflares reach the powers $10^{27} erg/s$ of microflares and produce the isolated turbulent events and high velocity jets observed by Brueckner and Bartoe (1983). Parker suggests that the observed X-ray corona is simply the superposition of a very large number of nanoflares.

In addition to the above discussed individual small scale or intermittent flows the chromospheres and coronae are the seat of systematic large scale persistent stellar wind flows which emerge from the open magnetic field configurations in coronal holes. These winds in solar-like stars are thermally driven, that is, the escape speed is close to the sound speed of the high-temperature coronae. For non-solar late-type giant stars, Alfvén wave driven winds are important. Even for the sun the momentum deposition due to Alfvén waves at distances greater than $15R_\odot$ (Withbroe 1988) is necessary to explain the observed interplanetary solar wind speed. For a review of late-type stellar winds see Dupree (1986) and Hammer (1989, this volume).

6. Conclusions

We have seen that chromospheres and coronae are layers with a unique physics. The uniqueness is due to their basic energetic support by mechanical heating, to the dominant influence of the magnetic fields, to their special geometry as stellar boundary layers with an NLTE thermodynamics, and to their function as source of eruptive type flows. Unfortunately the details of the mechanical heating are presently not well understood. Acoustic waves appear to play a significant role in stars of low rotation rate and as weak general background. The chromospheres and especially the coronae of more rapidly rotating stars are dominated by magnetic type heating: by acoustic-like slow-mode and Alfvén waves as well as by unsteady currents. Similarly, the role of the acoustic and magnetic mechanisms in driving eruptive flows is poorly known. Here more detailed stellar and particularly high-resolution solar observations are needed, together with more detailed theoretical developments of the various proposed heating mechanisms.

References

Anderson, L.S., Athay, R.G..: 1989, Astrophys. J., in press
Athay, R.G.: 1987, Nature **327**, 685
Athay, R.G., Gurman, J.B., Henze, W.: 1983, Astrophys. J. **269**, 706
Athay, R.G., Holzer, T.E.: 1982, Astrophys. J. **255**, 743
Avrett, E.H.: 1985, in: Chromospheric Diagnostics and Modelling, B.W. Lites Ed., Natl. Solar Observatory, Sunspot NM, p.67
Beckers, J.M.: 1972, Ann. Rev. Astron. Astrophys. **10**, 73
Bohn, H.U.: 1984, Astron. Astrophys. **136**, 338
Brueckner, G.E.: 1981, in Solar Active Regions, F.Q. Orrall Ed., Colorado Ass. Univ. Press, Boulder CO, USA, p. 113
Brueckner, G.E., Bartoe, J.D.F.: 1983, Astrophys. J. **272**, 329
Cuntz, M.: 1987, Astron. Astrophys. **188**, L5
Cuntz, M., Ulmschneider, P.: 1988, Astron. Astrophys. **193**, 119
Dahlburg, R.B., Dahlburg, J.P., Mariska, J.T.: 1988, Astron. Astrophys. **198**, 300
Dahlburg, R.B., Dahlburg, J.P., Mariska, J.T.: 1988, Astron. Astrophys. **198**, 300
Deubner, F.-L., Reichling, M., Langhanki, R.: 1988, in Advances in Helio- and Asteroseismology, IAU Symp. **123**, J. Christensen-Dalsgaard, S. Frandsen Eds., p. 439
Doschek, G.A., Feldman, U., Bohlin, J.D.: 1976, Astrophys. J. **205**, L177
Dupree, A.K.: 1986, Ann. Rev. Astron. Astrophys. **24**, 377
Elgarøy, Ø.: Astron. Astrophys. **204**, 147
Feldman, U., Cohen, L., Doschek, G.A.: 1982, Astrophys. J. **255**, 325

Gebbie, K.B., et al.: 1981, Astrophys. J. **251**, L115
Grossmann, W., Smith, R.A.: 1988, Astrophys. J. **332**, 476
Habbal, S.R., Leer, E., Holzer, T.E.: 1979, Solar Phys. **64**, 287
Hammer, R.: 1987, in: Solar and Stellar Physics, E.H. Schröter, M. Schüssler Eds., Lecture Notes in Physics **292**, Springer, Berlin, Germany, p. 77
Hammer, R., Ulmschneider, P.: 1989, Astron. Astrophys., in press
Herbold, G., Ulmschneider, P., Spruit, H.C., Rosner, R.: 1985, Astron. Astrophys. **145**, 157
Heyvaerts, J., Priest, E.R.: 1983, Astron. Astrophys. **117**, 220
Ionson, J.A.: 1978, Astrophys. J. **226**, 650
Ionson, J.A.: 1984, Astrophys. J. **276**, 357
Jordan, C., Linsky, J.L.: 1987, in: Chromospheres and Transition Regions, Y. Kondo Ed., D. Reidel, Dordrecht, p.259
Judge, P.G.: 1989, in The Evolution of Peculiar Red Giant Stars, IAU Coll. **106**, in press
Kalkofen, W., Ulmschneider, P., Schmitz, F.: 1984, Astrophys. J. **287**, 952
Linsky, J.L.: 1980, Ann. Rev. Astron. Astrophys. **18**, 439
Linsky, J.L.: 1988, in: Multiwavelength Astrophysics, F. Cordova Ed., Cambridge Univ. Press, p. ?
Middelkoop, F.: 1982, Astron. Astrophys. **113**, 1
Narain, U., Ulmschneider, P.: 1989, Space Science Reviews, in press
Oranje, B.J., Zwaan, C.: 1985, Astron. Astrophys. **147**, 265
Pallavicini, R., Golub, L., Rosner, R., Vaiana, G.S., Ayres, T., Linsky J.L.: 1981, Astrophys. J. **248**, 279
Parker, E.N.: 1983, Astrophys. J. **264**, 642
Parker, E.N.: 1986, in Coronal and Prominence Plasmas, A.I. Poland Ed., NASA CP-2442, p. 9
Parker, E.N.: 1988, Astrophys. J. **330**, 474
Rutten, R.G.M.: 1986, Astron. Astrophys. **159**, 291
Rutten, R.G.M.: 1987, Astron. Astrophys. **177**, 131
Schrijver, C.J.: 1983, Astron. Astrophys. **127**, 289
Schrijver, C.J.: 1987a, Astron. Astrophys. **180**, 241
Schrijver, C.J.: 1987b, in Cool Stars, Stellar Systems and the Sun, J.L. Linsky, R.E. Stencel Eds., Lecture Notes in Physics **291**, Springer, Berlin, Germany, p. 135
Schrijver, C.J., Coté, J., Zwaan, C., Saar, S.H.: 1989, Astron. Astrophys. **337**, 964
Stenflo, J.O.: 1978, Rep. Prog. Phys. **75**, 3
Stepien, K., Ulmschneider, P.: 1989, Astron. Astrophys. **216**, 139
Ulmschneider, P.: 1970, Solar Phys. **12**, 403
Ulmschneider, P.: 1986, Adv. Space Res. **6**, No. 8, 39
Ulmschneider, P.: 1988, Astron. Astrophys. **197**, 223
Ulmschneider, P.: 1989, Astron. Astrophys. in press
Ulmschneider, P., Muchmore, D.: 1986, in Small Scale Magnetic Flux Concentrations in the Solar Photosphere, W. Deinzer, M. Knölker, H.H. Voigt Eds., Vandenhoeck and Ruprecht, Göttingen, Germany, p. 191
Ulmschneider, P., Zähringer, K., Musielak, Z.: 1989, Astron. Astrophys., in press
Vaiana, G.S., et al.: 1981, Astrophys. J. **245**, 163

Van Ballegooijen, A.A.: 1986, Astrophys. J. **311**, 1001
Vernazza, J.E., Avrett, E.H., Loeser, R.: 1981, Astrophys. J. Suppl. **45**, 635
Vilhu, O.: 1987, in Cool Stars, Stellar Systems and the Sun, J.L. Linsky, R.E. Stencel Eds., Lecture Notes in Physics **291**, Springer, Berlin, Germany, p. 110
Walter, F.M., Schrijver, C.J.: 1987, in Cool Stars, Stellar Systems and the Sun, J.L. Linsky, R.E. Stencel Eds., Lecture Notes in Physics **291**, Springer, Berlin, Germany, p. 262
Wentzel, D.G.: 1974, Solar Phys. **39**, 129
Wilson, O.C., Bappu, M.K.V.: 1957, Astrophys. J. **125**, 661
Withbroe, G.L.: 1988, Astrophys. J. **325**, 442
Withbroe, G.L., Noyes, R.W.: 1977, Ann. Rev. Astron. Astrophys. **15**, 363
Zähringer, K., Ulmschneider, P.: 1987, in The Role of Fine- Scale Magnetic Fields on the Structure of the Solar Atmosphere, E.H. Schröter, M. Vazquez, A.A. Wyller Eds., Cambridge Univ. Press, Cambridge, England, p. 243
Zwaan, C.: 1978, Solar. Phys. **60**, 213